O adsorption and incipient oxidation of the Mg(0001) surface

Elsebeth Schröder,[1] Roman Fasel,[2] and Adam Kiejna[3]
[1]*Department of Applied Physics, Chalmers University of Technology and Göteborg University, SE-41296 Göteborg, Sweden*
[2]*Swiss Federal Laboratories for Materials Testing and Research (EMPA), nanotech@surfaces Laboratory, Feuerwerkerstrasse 39, CH-3602 Thun, Switzerland*
[3]*Institute of Experimental Physics, University of Wrocław, Plac M. Borna 9, PL-50-204 Wrocław, Poland*
(Received 30 June 2003; revised manuscript received 22 January 2004; published 29 March 2004)

First-principles density-functional calculations are used to study the early oxidation stages of the Mg(0001) surface for oxygen coverages $1/16 \leqslant \Theta \leqslant 3$ monolayers. It is found that at very low coverages O is incorporated below the topmost Mg layer in tetrahedral sites. At higher oxygen load the binding in on-surface sites is increased but at one monolayer coverage the on-surface binding is still about 60 meV weaker than for subsurface sites. The subsurface octahedral sites are found to be unfavorable compared to subsurface tetrahedral sites and to on-surface sites. At higher coverages oxygen adsorbs both under the surface and up. Our calculations predict island formation and clustering of incorporated and adsorbed oxygen in agreement with previous calculations. The calculated configurations are compared with results from angle-scanned x-ray photoelectron diffraction experiments to determine the geometrical structure of the oxidized Mg(0001) surface.

DOI: 10.1103/PhysRevB.69.115431 PACS number(s): 81.65.Mq, 68.43.−h, 61.14.Qp

I. INTRODUCTION

The process of oxidation of metal surfaces is of considerable fundamental scientific interest as well of paramount technological importance.[1] Corrosion and passivation are just two examples of either destructive or useful processes linked directly to this phenomenon, which are well known from everyday life. Oxidation of metal surfaces begins with dissociative chemisorption of oxygen on a clean surface and is followed by the formation of a film of metal oxide. In between these events there are many elementary processes. The study of Al and Mg oxidation is particularly important because Al and Mg belong to the group of so-called simple metals and are considered model systems for studies of oxidation of transition metals. Both metals exhibit high reactivity with oxygen and oxidize rapidly. Aluminum oxides (alumina) form several different phases where the structure of some of them was only recently identified by combined *ab initio* density-functional theory (DFT) and experimental studies.[2] Magnesium oxide is known to eventually form crystals of the rocksalt structure,[3] but can also experience complex reconstructions at partial coverages.[4,5] Both Mg and Al oxides play an important role in catalyst support and find many other useful applications.

The number of experimental[5–15] studies and theoretical[4,16] treatments devoted to the oxidation of magnesium is relatively limited compared to the more extensively studied oxidation of aluminum. In this paper we present a systematic study of the initial oxygen incorporation and island formation by first-principles theory calculations and we use the results to interpret high-quality x-ray photoelectron diffraction (XPD) measurements for low O_2 doses.

The existing picture of the Mg(0001) surface oxidation processes dates back to the early 1980s. Based on the extensive low-energy electron diffraction (LEED), Auger electron spectroscopy, electron energy-loss spectroscopy, and work function measurements Namba *et al.* proposed[6] a four-stage model consisting of: (1) dissociative oxygen chemisorption at random sites followed by oxygen incorporation, (2) assembly of incorporated oxygen atoms into islands and lateral growth, (3) oxide formation from surface Mg atoms and subsurface O atoms which starts at O_2 exposures around 2–3 L (Langmuir) or 0.5–1 monolayer of total coverage, and (4) oxide thickening. Several other experimental studies provided arguments for a three-stage model of oxidation that was proposed at approximately the same time. In this model[9,10] atomic oxygen is directly incorporated into magnesium (below the top Mg layer) right after on-surface dissociation. In the next step there is simultaneous formation of an oxide layer and a decrease in the oxygen on the surface.[10] Finally, there is oxide thickening and transformation into a rocksalt structure.

This model of immediate incorporation of oxygen gained support from the x-ray photoelectron spectroscopy study of Ghijsen *et al.*,[7] and particularly from the measured sharp decrease in the work function of the Mg(0001) surface upon initial O exposure.[8] The formation of an O-(1×1) subsurface layer up to monolayer coverage and its subsequent transformation into epitaxial oxide was also reported.[8] The positions of the subsurface oxygen atoms were deduced to be octahedrally coordinated where the oxygen has an environment similar to that in MgO.[10] This is in agreement with a more direct experimental evidence for oxygen incorporation in the octahedral interstitial sites of the first two interlayer spacings of Mg during the initial stages of magnesium oxidation,[11] and with later inelastic ion scattering experiments on a polycrystalline Mg surface.[14,15] A recent scanning tunneling microscopy (STM) study of the oxidation of Mg(0001) suggests that at low oxygen exposures (up to 2 L) the incorporated oxygen atoms form a single layer underneath the top layer of Mg.[5] The idea of immediately populated subsurface sites seems also to be supported by recent measurements by Mitrovic *et al.*,[12] however, they show that most of the oxygen (90%) remains over the surface and only a small fraction goes below the surface. Thus, the question

regarding the most favored adsorption sites is still debated and requires further analysis.

On the theoretical side, the local-density-functional theory (DFT) calculations of Bungaro *et al.*[16] show that oxygen is incorporated forming a (1×1) subsurface lattice. A recent DFT-based lattice gas model study[4] of island formation in the early Mg(0001) oxidation stages has shown that at very low filling the oxygen atoms adsorb in the top-most subsurface (tetrahedral) B sites in an ABAB . . . stacking of magnesium. At higher oxygen load also the deeper sites are filled, and the adsorbed oxygen atoms form dense clusters just below the surface and in further subsurface locations.[4,16] For larger clusters the oxygen-oxygen interaction effects drive the oxygen atoms further into the magnesium subsurface layers and bulk.

The rest of this paper is organized as follows. In Sec. II systematic DFT calculations in the range of coverages between 1/16 and 3 monolayers (ML) are presented. In Sec. III we describe our high-quality XPD measurements for low O_2 doses, and in Sec. IV our DFT results are used to interpret the experimental XPD data.

II. THEORY

The calculations are carried out using the plane-wave density-functional DACAPO code[17] with the generalized gradient approximation (GGA) for the exchange-correlation energy functional[18] and with ultrasoft pseudopotentials[19] to represent the ionic cores. The clean Mg(0001) surface is modeled by periodic slabs consisting of six to seven magnesium layers separated by 21 Å of vacuum. The plane-wave basis set with 25 Ry energy cutoff is used. This slab thickness, amount of vacuum, and the chosen energy cutoff was shown to give well-converged binding-energy values. The O atoms are adsorbed on one side of the slab only and the electric field arising due to the asymmetry of the system is compensated for by a consistent dipole correction.[20,21] A $4\times4\times1$ mesh of Monkhorst-Pack special k points for the 4×4 atom surface unit cell and a Fermi-surface smearing of 0.2 eV are applied to the Brillouin-zone integrations. For smaller cells the number of k points are increased accordingly up to a $16\times16\times1$ mesh for the 1×1 surface unit cell. The positions of atoms in the three to four topmost magnesium layers, and of all the oxygen atoms, are fully optimized until the sum of the Hellmann-Feynman forces on all unconstrained atoms converges to less than 0.05 eV/Å. The forces acting on the ions in the unit cell are derived from the converged charge densities, and the atom dynamics is determined using a preconditioned quasi-Newton method based on the Broyden-Fletcher-Goldfarb-Shanno algorithm.[22]

The calculated lattice constants for hcp Mg is $a=3.19$ Å and $c/a=1.64$, which agree very well with the experimental values 3.21 Å and 1.623 (Ref. 23) and other GGA calculations.[24] The bulk modulus, ignoring lattice vibrations, is found to be 34.1 GPa,[25] in good agreement with the measured value 35.5 GPa (obtained from the elastic constants of Ref. 26) and with the GGA calculations of Ref. 24.

For the bare-metal surface the relaxations of the interlayer spacing with respect to the bulk spacing show 1.5% expansion, 0.4% contraction, and 1.3% contraction of the first, second, and third interlayer distance, respectively. The expansion of the first interlayer distance compares well with the experimental[27] value of 1.7%, and with other GGA calculations.[24] The small contraction of the second spacing disagrees with a small expansion predicted by experiment and other calculations. Since the magnitude of this relaxation is very small this discrepancy should not have any significant effect on the results for O adsorption. The calculated work function is 3.72 eV for the relaxed surface and agrees well with the experimental value 3.84 eV.[28]

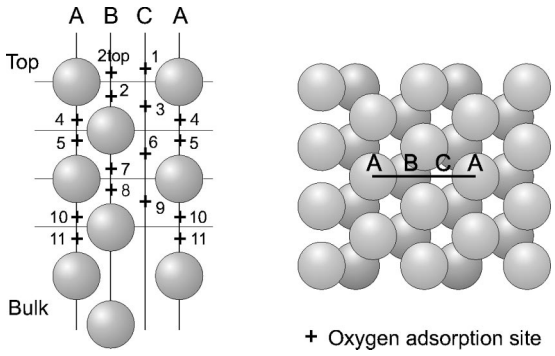

FIG. 1. Sketch of the adsorption sites of oxygen at low coverage. The positions indicated by crosses to the left are the adsorption sites at 1/16 ML single O-atom adsorption.

A. Low coverages ($\Theta\leqslant0.5$) of oxygen

The locations of the possible on-surface and subsurface adsorption sites of Mg(0001) considered in our calculations are sketched in Fig. 1. The results for single or nearest-neighbor pairs of O atoms adsorbed at the 4×4, 2×2, and 1×2 surface cells were used as 1/16, 1/8, 1/4, and 1/2 ML coverage data.

In Fig. 2 we present the low-coverage binding energies calculated relative to the energy of an isolated, spin-

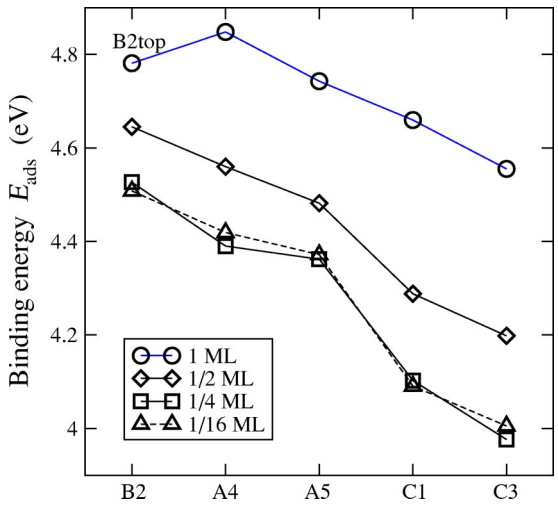

FIG. 2. The calculated low-coverage binding energies for different adsorption sites as indicated in Fig. 1. For 1 ML coverage the B2 site is replaced by the slightly on-surface site B2top. For coverages $\Theta\leqslant0.5$ ML the only stable on-surface site is $C1$.

polarized O_2 molecule and the clean, relaxed Mg surface. The convergence tests with respect to the size of unit cell and the number of *k* points show that the error bars for the binding energy do not exceed 10 meV. The positional changes of the Mg atoms induced by adsorption of oxygen are in most cases not very large. For the 2×2 supercell with a single O atom slightly below the surface (site B2 in Fig. 1) or in first-sublayer adsorption sites (sites A4 or A5) the Mg atoms move less than 3% vertically and 0.6% laterally from their clean-surface positions. To estimate the sensitivity of the binding energy to positional relaxations of the atoms we also calculated the binding energy of an even distribution of four O atoms in the tetrahedral subsurface sites B2 in the 4×4 system, and of one site-B2 atom in the 2×2 system. The two configurations (converged within the force requirement) relax to slightly different atomic positions which differ by 5 meV. We therefore estimate the relaxation-imposed inaccuracy of the binding energies to be approximately 5 meV.

The calculated binding energies (Fig. 2) show that for single atom adsorption at coverages $\Theta\leqslant0.5$ (corresponding to a single O atom in the 4×4, 2×2, and 1×2 surface unit cells) the only stable on-surface adsorption site is the fcc hollow denoted as C1 (Fig. 1), and the binding energy of this site is significantly less than that of any of the subsurface sites. We find *no* single-adsorbant energy minimum near the position where we would expect the other natural candidate, the on-surface B2top site. Instead, when relaxing dilute systems with O in the B2top sites the surrounding Mg atoms move laterally by a small amount, enough to let the O-atoms sink into the subsurface B2 (tetrahedral) site. Only if a pair of O atoms are adsorbed as nearest neighbors, or at increased O loading ($\Theta\geqslant1$), can one of the O atoms be stabilized on the surface in the B2top site. These results are in agreement with the findings of Bungaro *et al.*[16] as to subsurface adsorption sites being more favorable than on-surface ones, but contradict their prediction of a stable on-surface B2top site for low coverages. However, for coverages $\Theta<1$ their *k*-point sampling was limited to the Γ point only.

By extensive searches for subsurface adsorption sites we find that within the two top Mg layers the tetrahedral (B2, A4, and A5) sites have higher binding energies than the on-surface C1 and the subsurface octahedral C3 site for all coverages $\Theta\leqslant0.5$ (compare Fig. 2 and Table I). Thus, in the oxidation process the first O atom adsorbs in a subsurface site of type B2, its binding energy being only 0.09 eV and 0.15 eV higher (Fig. 2) than that of O in subsurface site A4 and A5, respectively. The preference for the B2 site agrees with the results of Ref. 16, but we find a binding energy 0.15–0.47 eV larger at coverages $1/16\leqslant\Theta\leqslant1/2$.

We checked the possibility of forming ionic complexes consisting of the Mg atoms of the topmost layer and subsurface and on-surface oxygen (which would represent a seed for further oxide formation), by searching for the most preferred sites for an O atom additional to the one preadsorbed in a B2 site. As is evident from Table I, even at very low coverages, the addition of another O atom leads to an increased O population in the B2 sites. The two (neighboring) atoms in the B2 sites are by ~0.03–0.04 eV more favored than one atom in the B2 site and another one in either the A4 or A5 site.

TABLE I. The binding energy E_{ads} per O atom for a double-site O occupancy of different chemisorption sites (see Fig. 1) and for different surface unit cells. Two O atoms in the 4×4 and 2×2 surface unit cells correspond to the coverages $\Theta=1/8$ and 1/2, respectively. The exact vertical position of the sites B2 are distinguished by ''top'' for a position (slightly) above the top Mg layer, and ''mix'' for a position in which some of the top Mg atoms are above and some are below the oxygen atom, whereas B2 denotes adsorption below all atoms of the top-most Mg layer. All pairs of sites are nearest neighbors.

Sites	E_{ads} (eV)
1/8 ML coverage	
B2 and B2	4.58
B2 and C3	4.28
B2 and A4	4.55
B2 and A5	4.54
B2top and B2	4.51
1/2 ML coverage	
B2 and B2	4.64
B2mix and C3	4.26
B2mix and A4	4.51
B2 and A5	4.51

In summary, we find the initial oxygen adsorption to be a subsurface process. A previously suggested preferential adsorption into *on-surface* sites for low O coverages,[12] as is the case for, e.g., oxygen adsorption on Al(111),[29] is not supported by our results.

B. Higher oxygen coverage ($1\leqslant\Theta\leqslant3$ ML)

For 1 ML coverage, considering only single-site occupation, the energetic ordering of the most stable sites changes (Fig. 2 and Table II). The B2-type sites become less favorable than the subsurface tetrahedral A4 site and the actual B2 site is shifted to the B2top position. However, allowing for simultaneous occupancy of the B2 and B2top sites at 1 ML in the 1×2 unit cell (Table II) we find that this combined B-site structure is by 0.06 eV more favored than the single A4 occupancy shown in Fig. 2.

As more oxygen is adsorbed into the Mg surface the possible adsorbate configurations grow in number, partly due to simple combinatorics, and partly because new adsorption sites appear within an increasingly distorted Mg background lattice. This is already apparent for nearest-neighbor adsorption in the low-coverage region (Table I) where a slight vertical distortion of the top Mg layer in some cases leads to adsorption in the B2top site and in a ''mixed'' B2-B2top position. In Table II we name the 1 ML configurations by the adsorbate position, but for higher coverages the notation is merely an approximate description of the structure, and we refer the reader to Fig. 3 for a sketch of the multitude of similar but not identical configurations at coverages 2–3 ML's.

TABLE II. The binding energy E_{ads} per O atom, work function change $\Delta\Phi$, and the experimental XPD reliability factor R_{MP} in different chemisorption sites for 1–3 ML oxygen coverage. For calculations involving sites within the third Mg layer and below it (sites B7, B8, A10, and A11) one extra layer of relaxed Mg atoms was added to the slab, which then has totally 7 layers of Mg of which the four top-most layers are relaxed. This resulted in a small increase of the E_{ads} of the order of 5 meV but has not changed the ordering of energies of the sites. Please refer to Fig. 3 for our naming of the 2–3 ML structures.

Sites	E_{ads} (eV)	$\Delta\Phi$ (eV)	R_{MP} (1.4 L)	R_{MP} (9.7 L)
1 ML, nearest neighbors				
B2 and A5	4.76	−0.64	0.41	0.30
B2mix and A4	4.72	−0.62	0.34	0.37
B2top and C3	4.55	−0.49	0.51	0.43
1 ML, one atom per unit cell				
B2top and B2	4.90	−0.46	0.46	0.46
A4	4.85	0.00	0.42	0.48
B2top	4.78	−0.99	0.44	0.46
A5	4.74	0.11	0.53	0.42
C1	4.66	−0.12	0.44	0.46
C3	4.56	0.62	0.56	0.51
2 ML				
A4 + B7	5.12	−0.07	0.41	0.50
A5 + B8	5.07	0.27	0.56	0.45
B2 + A5	5.05	−0.03	0.44	0.33
Rocksalt 2ML	4.96	0.72	0.54	0.45
Flat 2ML	4.93	−1.14	0.29	0.36
3 ML				
A4 + B7 + A10	5.22	0.04	0.45	0.50
A5 + B8 + A11	5.18	0.09	0.53	0.43
B2 + A5 + B8	5.17	0.04	0.46	0.35
Rocksalt 3ML	5.12	0.78	0.55	0.50
Flat 3ML	4.99	−1.14	0.30	0.37

The stable structures found in the 2 and 3 ML coverage region (Table II) fall in two general classes: layered ones with O and Mg in buckled or flat layers of a hexagonal pattern [Fig. 3(a)–3(c), and 3(e)], and rocksalt structures [Fig. 3(d)] on top of clean magnesium, strained with respect to the clean-surface lattice constant. The layered structures can be described as a Mg(0001) surface with slightly changed atomic positions to accommodate O atoms within the top Mg layers. Each of the layers has a honeycomb structure with O at every second vertex and Mg at the remaining vertices. The layers are stacked in an AA′ stacking sequence, with O on top of Mg atoms and *vice versa* at a layer separation of approximately 2.3–2.7 Å. The buckled structures, which involve subsurface oxygen only, are buckled up or down, depending on the oxygen atoms staggering over or below the Mg layer, respectively. The vertical separation of O and Mg within a buckled layer [Fig. 3(a)–3(c)] is $\approx$0.6 Å. The flat structures [Fig. 3(e)] have vertical O-Mg separations of 0.01–0.06 Å and do not exist as subsurface layers. In these phases the top-most oxygen atom sits slightly above the top Mg layer, corresponding approximately to the position of site B2top in Fig. 1. Again, we find (Fig. 3) that subsurface layered structures are preferred. It is evident that with increased O coverage, the difference in binding energies (Fig. 3) for the subsurface layered and rocksalt phases is diminishing, indicating that eventually, for still higher coverage, the rocksalt structure may become the most favorable one. Note that for several other configurations with 2 ML or 3 ML coverage of the tetrahedral adsorption sites (not listed in Table II) no energy minimum is found. This includes any flat subsurface structures, phases of mixed flat and buckled layers, and mixed buckled-up and buckled-down layers. Further, we also tested structures that include an octahedral (C3, C6,C9) site in the 2 ML and 3 ML coverage range, but found binding energies per atom at least 0.3–0.4 eV smaller than the energetically best structures at the same coverage, similar to our low-coverage results (Fig. 2).

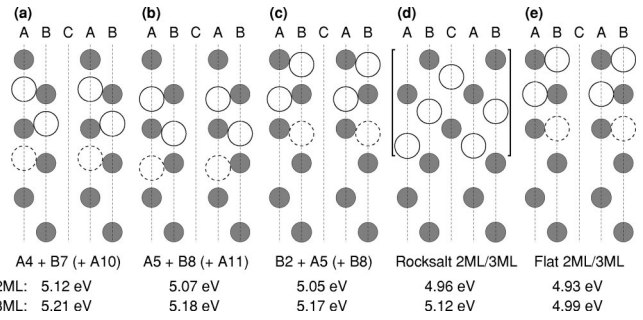

FIG. 3. Schematic plot of the 2–3 ML structures, cut along the ABCAB line in Fig. 1, and their binding energies. Small gray circles are Mg atoms, large white circles are O atoms. The dashed circles indicate O atoms that are only included in the 3 ML structure. The buckling of the Mg-O layers in (a)–(c) is exaggerated. For the rocksalt structure only the 3 ML structure is shown, and the oxide structure is in brackets to indicate that the atoms are shifted out of the cut plane. The rocksalt structure has the atoms of the third Mg layer, counted from the top, sitting on a bridge site of the fourth Mg layer. The structures are in order of decreasing binding energy E_{ads}.

Table II only presents the energetically most favored structures of all the configurations calculated by us. These structures are close in binding energy and since in reality a system does not always find its minimum-energy configuration, due to kinetics, barriers, etc., we also calculated the corresponding work function for comparison with experiments (Table II). Originally, an experimentally observed sharp work function decrease upon oxidation suggested the preference for subsurface adsorption at the Mg(0001) surface.[8] Previous local-density-approximation DFT calculations[16] have shown that only oxygen incorporation into B2 sites lowers the work function, and for 1 ML load this lowering was found to be 0.3 eV, which is much smaller than measured experimentally. We do not find 1 ML adsorption in the B2 sites, but by considering also the neighboring B2top sites our results (Table II) confirm the lowering of the work function, although with a larger value. Keeping in mind that the oxygen atoms show a tendency of clustering, higher coverages than 1 ML should also be considered when comparing to experimental measurements, even if the global cov-

erage is small. We find from our calculations that in addition to the 1 ML B2top structure, the flat 2 ML and 3 ML structures also exhibit a work function change of about -1 eV, which agrees very well with the value found in recent measurements.[12] Thus, the work function results and binding energy calculations show that the flat 2 ML and 3 ML structures are the ones found in physical reality.

It is generally expected that an adlayer of negative O ions will increase the metal-surface dipole layer and hence the work function. For example, this is clearly the case for oxygen on the Al(111) surface.[29] Our results suggest that on-surface oxygen on the Mg(0001) surface, either as 1 ML B2top or as flat 2 ML or 3 ML structures, leads to a decrease in the work function consistent with experimental observations.[12] On the other hand, neither the 1 ML B2top sites nor the flat 2 ML or 3 ML structures are the energetically most favorable at the given coverages. Binding energy considerations show the combined B2 and B2top structure to be more favorable at 1 ML, with a smaller work function change, and subsurface structures to be more favorable at 2 ML and 3 ML, with small negative or even slightly positive work function changes. In Ref. 16 it was suggested that a sufficiently high-energy barrier for moving an O atom from the surface and into the subsurface sites might require the O atoms to stay on the surface instead of adsorbing into the energetically more favorable subsurface sites. We tested this suggestion by calculating the energy barrier from the B2top site to the A4 site at 1 ML coverage and found the barrier height to be 0.35 eV per O atom. This is enough to prevent an O atom from moving to a more favored site at the low (zero) temperature of the DFT calculations but is not sufficient to keep the O atoms on surface at macroscopic time scales at room temperature.

At low coverage the only on-surface sites are the fcc hollows (C1), but also the lower-lying subsurface B2 sites are exposed to O atoms arriving at the surface. Thus, we conjecture that an O-atom arriving at the surface will find the B2 site having a higher binding energy than the C1 site and will immediately diffuse to the former. The B2 sites are most favorable up to 0.5 ML coverage (Fig. 2). With growing O coverage the energetic situation changes and the deeper tetrahedral sites become more favorable. As we have seen, the energy barrier to overcome is not enough at room temperature to stop the diffusion of O atoms into the surface, and thus energy arguments predict subsurface adsorption. It is up to discussion why the work function change calculations, and to some extent our XPD experiments presented in Sec. III, favor the metastable on-surface occupation (with additional O atoms in subsurface sites). However, both our energy considerations, our work function calculations, and as shown later our XPD experiments very clearly exclude any possibility of a rocksalt surface structure and point to layered structures at 2–3 ML coverage.

Figure 4 displays an interesting comparison of the electron charge redistribution for three of the 2 ML structures. Whereas the rocksalt structure [Fig. 4(b)] has an almost isotropic charge distribution around each atom, as is typical for ionic binding, the two layered structures show a more complicated, anisotropic picture. The flat layered structure [Fig. 4(c)] shows most clearly a directional bonding, with more charge redistribution along the in-plane nearest-neighbor Mg-O lines than in other directions.

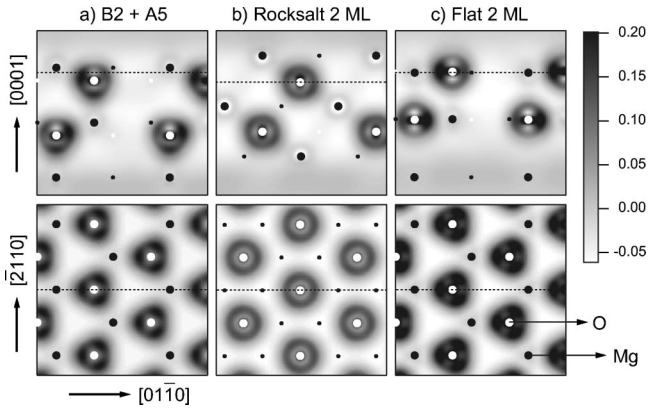

FIG. 4. The electron charge redistribution due to the presence of the O atoms. Shown are the three 2 ML structures that have O atoms closest to the surface, cut in the $[2\bar{1}\bar{1}0]$ direction perpendicular (top panels) and parallel to the surface (bottom panels). Atomic positions are indicated by white (O) and black (Mg) dots. The change in electron density distribution is $\Delta n(\mathbf{r}) = n^{\mathrm{Mg+O}}(\mathbf{r}) - n^{\mathrm{Mg}}(\mathbf{r}) - n^{\mathrm{O}}(\mathbf{r})$ where $n^{\mathrm{Mg+O}}$ is the electron density for the full system, n^{Mg} the electron density in the absence of O atoms, and n^{O} the atomic O charge density. A negative/positive Δn corresponds to a depletion/accumulation of electrons (in units of $e/\mathrm{Å}^3$).

Island formation. It was shown previously[4] that oxygen atoms adsorbed in the Mg(0001) surface form dense clusters in tetragonal subsurface sites. In the present investigation we find that the O atoms show a tendency for island formation by pairing up in combinations with subsurface sites. Figure 2 and Table I show that the higher the coverage, the larger the binding energy of the lower-lying sites (sites A4 and A5). In general, the binding energy is higher in more close-packed systems, thus showing that clusters or islands of O atoms are preferred to isolated or pairs of O atoms.

The preference for subsurface island formation in tetrahedral A4, or lower, sites agrees with theoretical simulations.[4,16] A new feature not observed in Ref. 16 is the appearance of the on-surface O islands for 1 ML coverage. We also note that the binding-energy differences for oxygen in different sites are relatively small for $\Theta = 1$. The tendency to form islands continues with further increase of coverage, showing some quenching in the binding energy at 3 ML coverage, in agreement with Ref. 4.

III. EXPERIMENTS

To supplement the DFT calculations and to provide a reference ground we have also carried out XPD measurements of the clean Mg(0001) surface and after low dosing of oxygen.

A. Method

XPD has been chosen because of its chemical sensitivity and its sensitivity to local real space order. It is a powerful technique for surface structural investigations,[30] and it has

been shown that full-hemispherical XPD patterns provide very direct information about the near-surface structure. At photoelectron kinetic energies above about 500 eV, the strongly anisotropic scattering by the ion cores leads to a forward focusing of the electron flux along the emitter-scatterer axis. The photoelectron angular distribution, therefore, is to a first approximation a forward-projected image of the atomic structure around the photoemitters. Analysis of the symmetry and positions of forward-focusing maxima thus permits a very straightforward structural interpretation of XPD data. Furthermore, detailed structural parameters can be determined by comparing the experimental XPD patterns to calculated ones. The relatively simple and efficient single-scattering cluster (SSC) formalism[30] has proven adequate in most cases. The agreement between SSC calculations and experimental XPD pattern can be quantified using a reliability factor such as the R factor R_{MP} defined previously.[31,32]

The experiments have been performed in the University of Fribourg's VG ESCALAB Mk II spectrometer modified for motorized sequential angle-scanning data acquisition. Clean Mg(0001) surfaces have been prepared by cycles of sputtering (500 eV Ar^+) and annealing (130 °C). Before O_2 exposure, the surface displayed a sharp (1×1) LEED pattern with little background. After O_2 exposure with the sample held at room temperature, the coverage was determined from the relative intensities of the O 1s and Mg 2p photoelectron peaks. Experimental O 1s XPD patterns were obtained after exposure of the Mg(0001) surface to 0.15, 0.7, 1.4, and 9.7 L of O_2, corresponding to *global* O coverages of 0.1, 0.4, 1, and 1.7 ML, respectively.

B. Oxygen adsorbed at Mg(0001)

The Mg(0001) surface with various coverages of oxygen atoms was studied with LEED and XPD. Experimental XPD patterns for O_2 doses of 0.15 and 9.7 L are shown in Fig. 5. The most prominent feature of the 0.15 L pattern is a strong intensity maximum at normal emission. This observation is a clear and direct evidence for O adsorption below the topmost Mg layer: Only an atom located directly above the oxygen photoelectron emitter can give rise to a forward-focusing maximum at normal emission, i.e., in the center of the plot. A further conclusion can immediately be drawn from the evolution of the XPD pattern with O_2 exposure. Apart from differences due to counting statistics, the experimental XPD patterns are strikingly similar, not only regarding the intensity maximum at normal emission but regarding all the prominent diffraction features. It must therefore be concluded that the local atomic geometry is the same over the entire exposure range.

The same conclusion is obtained from the evolution of the LEED pattern with increasing O_2 exposure: The LEED pattern stays (1×1), and only the background rises slightly, which indicates an increasing amount of disorder with increasing coverage. Since no superstructures are observed, the presence of any other islands than islands of (1×1) periodicity that are larger than about 50–100 Å can therefore be excluded.

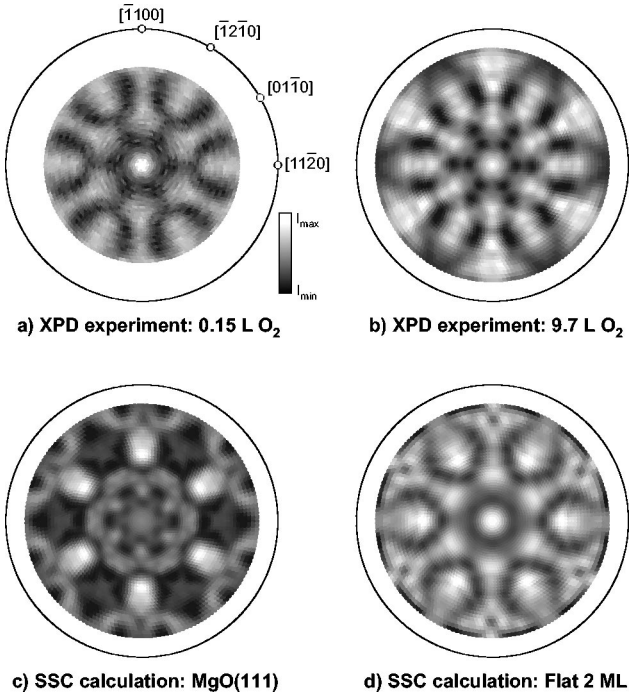

FIG. 5. Experimental O 1s XPD patterns after exposures of the Mg(0001) surface to (a) 0.15 L and (b) 9.7 L of oxygen. (c) SSC calculation for the MgO(111) rocksalt structure. (d) SSC calculation for the 2 ML layered oxide structure ("Flat 2 ML") yielding best agreement with the experimental 1.4 L XPD pattern.

In other words, both the LEED and XPD measurements indicate that locally the geometry is the same irrespective of the global coverage (at least below 1.7 ML). Already at 0.1 ML global coverage this local structure thus contains at least 1 ML oxygen, and with increasing coverage it will grow in domain size without significant changes in geometrical structure. Therefore, determining the local geometrical structure at 1 ML local coverage will determine the geometries even at the lowest global coverages accessible to the experiments.

In the further analysis we compare simulated SSC diffraction pattern to experimental XPD images of the Mg(0001) surface both with dosing 1.4 L (approx. 1 ML global coverage) and 9.7 L ($\approx$1.7 ML global coverage).

IV. COMPARISON BETWEEN EXPERIMENT AND THEORY

The O/Mg(0001) system does not simply form a MgO(111) rocksalt structure as is clearly seen by comparing a simulated diffraction pattern for MgO(111) [Fig. 5(c)] to the experimental 9.7 L XPD pattern shown in Fig. 5(b): The simulation does not reproduce any of the diffraction features satisfactorily. Therefore, the most relevant atomic structures, as determined by the DFT calculations, were used to simulate XPD patterns by means of SSC calculations. The resulting SSC calculations were compared to the experimental 1.4 L and 9.7 L XPD patterns, the latter of which is shown in Fig. 5(b).

None of the SSC calculations for an oxygen atom in an isolated site gave satisfactory agreement with experiment. The calculations, however, confirm the conclusion drawn from the experimental patterns that one oxygen atom is adsorbed directly below a Mg atom: Only the simulations for oxygen in the A4 and A5 sites exhibit the characteristic intensity maximum at normal emission that is seen in experiment [Figs. 5(a) and 5(b)]. The fact that the experimental XPD patterns do not agree with simulated diffraction patterns of disperse, low local coverages even for low overall coverage in the experiment is consistent with the LEED measurements discussed above, indicating again that the oxygen will form island with a local coverage of 1 ML or more. Accordingly, further SSC calculations concentrated on the atomic positions obtained from DFT calculations using a 1×1 surface cell.

Among the simulated diffraction patterns for 1 ML local coverage again only the site A4 and the site A5 SSC calculations exhibit a central maximum. In contrast, the SSC calculations for each of the C3, B2top, and C1 sites (leaving all other sites empty) do not show such maximum. This means that the comparison between SSC calculations and experimental XPD patterns disqualifies the site B2top-only occupation at 1 ML local coverage, in agreement with the theoretical binding energy being smaller for B2top than for A4 at 1 ML coverage. Along with the binding energy obtained from the DFT calculations the comparison to the XPD patterns also rules out octahedral subsurface (site C3) occupation.

Consequently, SSC calculations were also performed for the atomic positions obtained from DFT calculations considering 2 ML and 3 ML coverage. In Table II we summarize the 1 ML, 2 ML, and 3 ML local coverage SSC simulations [one to three O atoms per (1×1) cell] by listing their reliability factors with respect to the 1.4 L and 9.7 L exposure XPD data. Best agreements between experiment and SSC calculations (lowest reliability factors) are found for the layered structures ''B2mix and A4'' and ''B2 and A5'' at 1 ML local coverage, ''Flat 2 ML'' [Fig. 5(d)] and ''B2 + A5'' at 2 ML local coverage, and ''Flat 3 ML'' and ''B2 + A5 + B8'' for 3 ML local coverage. These results are consistent with the work function changes discussed above.

The general trend is that the rocksalt structures (2 ML and 3 ML) do not agree very well with the experimental XPD patterns (high values of R_{MP}), whereas some of the layered structures agree better. In particular we notice that among the 2 ML structures the flat structure (''Flat 2 ML'') has the best agreement with the 1.4 L experiment, whereas one of the buckled layer structures (''B2 + A5'') fits best to the 9.7 L experiment. This indicates that as the global coverage is increased by higher O_2 dosing, more of the surface becomes covered with buckled Mg and O layers and less with the flat surface.

For the 1.4 L dosing experiment the flat surface is favored, in disagreement with the DFT binding energy results, but in agreement with the calculated work function change. 1.4 L dosing corresponds to ~1 ML of global coverage, but since the distribution of oxygen is nonuniform due to the tendency of the atoms to form islands the experimentally observed surface is patched. For small surface oxide patches of 2 ML's (or more) local oxygen coverage the strain can get released over most of the island and thus, experimentally, mostly the flat structure is seen at low dosing. This gives a low R_{MP} value for the flat structure, but still keeps the order of the buckled and rocksalt structure found in DFT calculations: buckled is also at 1.4 L more favored experimentally than rocksalt. Thus, the relevant dosing (among the measured ones) to use for comparing DFT and the XPD experimental structures is 9.7 L. This structure probably does not fully cover the surface (if clusters are at least 2 ML dense), but certainly does so to a larger extent than for dosing 1.4 L. At dosing 9.7 L the DFT calculations and the XPD experiment agree on the buckled surface.

Based on both the calculated and experimental structures discussed above we conclude that at relatively low dosage (corresponding to 2–3 ML coverage) O/Mg(0001) forms the layered oxide structure. The rocksalt structure typical of MgO starts to grow only at higher O dosing.

V. SUMMARY AND CONCLUSIONS

We have performed extended first-principles calculations of oxygen adsorption and of the initial stages of Mg(0001) oxidation. A variety of configurations and a wide range of coverages were considered in order to determine the most stable structures. These were compared with x-ray photoelectron diffraction experiment and simulations. At low coverages ($\Theta\leqslant0.5$ ML) both our DFT calculations and experiment show that oxygen adsorbs in subsurface sites. Our DFT calculations show that the first O atom chemisorbed in the oxidation process binds in a subsurface tetrahedral site of the B2 type. At higher coverage O adsorbed in subsurface tetrahedral sites shows a tendency to form subsurface islands, resulting in an increased binding energy. For the 2 ML (3 ML) coverages we find some rather unanticipated surface oxide structures, consisting of two (three) mixed oxygen-magnesium layers on top of an almost undistorted Mg(0001) surface. These layered oxide structures have hexagonal symmetry and can be flat or buckled. We find that the rocksalt structure can be excluded at 2–3 ML coverage, both by binding energy arguments and by comparison to our XPD experiments. However, our DFT results also show that the rocksalt structure may become energetically competitive at an increased coverage.

ACKNOWLEDGMENTS

This work was supported in part by the Swedish Foundation for Strategic Research (SSF), the Swedish Research Council (VR), The Swedish Foundation for International Cooperation in Research and Higher Education (STINT), the Carl Tryggers Foundation, and the Polish State Committee for Scientific Research (KBN), Project No. 5 P03B 066 21. R.F. would like to thank P. Aebi for continuous support and help with the XPD experiments. The allocation of computer time at the UNICC facility at Chalmers and Göteborg University is gratefully acknowledged.

[1] *The Surface Science of Metal Oxides*, edited by V.E. Henrich and P.A. Cox (Cambridge University Press, Cambridge, 1994).
[2] Y. Yourdshahyan *et al.*, J. Am. Ceram. Soc. **82**, 1365 (1999).
[3] C. Noguera, J. Phys.: Condens. Matter **12**, R367 (2000).
[4] E. Schröder, Comput. Mater. Sci. **24**, 105 (2002).
[5] A.U. Goonewardene, J. Karunamuni, R.L. Kurtz, and R.L. Stockbauer, Surf. Sci. **501**, 102 (2002).
[6] H. Namba, J. Darville, and J.M. Gilles, Surf. Sci. **108**, 446 (1981).
[7] J. Ghijsen, H. Namba, P.A. Thiry, J.J. Pireaux, and P. Caudano, Appl. Surf. Sci. **8**, 397 (1981).
[8] B.E. Hayden, E. Schweizer, R. Kötz, and A.M. Bradshaw, Surf. Sci. **111**, 26 (1981).
[9] S.A. Flodström and C.W.B. Martinsson, Surf. Sci. **118**, 513 (1982).
[10] P.A. Thiry, J. Ghijsen, R. Sporken, J.J. Pireaux, R.L. Johnson, and R. Caudano, Phys. Rev. B **39**, 3620 (1989).
[11] H. Cronacher, K. Heinz, K. Müller, M.-L. Xu, and M.A. van Hove, Surf. Sci. **209**, 387 (1989).
[12] B.C. Mitrovic, D.J. O'Connor, and Y. Shen, Surf. Rev. Lett. **5**, 599 (1998).
[13] S.M. Driver, J. Lüdecke, G.J. Jackson, and D.P. Woodruff, J. Electron Spectrosc. Relat. Phenom. **98-99**, 235 (1999).
[14] S. Lacombe, L. Guillemot, and V.A. Esaulov, Surf. Sci. **304**, L431 (1994).
[15] V.A. Esaulov, O. Grizzi, L. Guillemot, M. Maazouz, S. Ustaze, and R. Verucchi, Surf. Sci. **380**, L521 (1997).
[16] C. Bungaro, C. Noguera, P. Ballone, and W. Kress, Phys. Rev. Lett. **79**, 4433 (1997).
[17] Computer code DACAPO, version 1.30, http://www.fysik.dtu.dk/CAMPOS/
[18] J.P. Perdew, J.A. Chevary, S.H. Vosko, K.A. Jackson, M.R. Pederson, D.J. Singh, and C. Fiolhais, Phys. Rev. B **46**, 6671 (1992); **48**, 4978(E) (1993).
[19] D. Vanderbilt, Phys. Rev. B **41**, 7892 (1990).
[20] J. Neugebauer and M. Scheffler, Phys. Rev. B **46**, 16 067 (1992).
[21] L. Bengtsson, Phys. Rev. B **59**, 12 301 (1999).
[22] W.H. Press, B.P. Flannery, S.A. Teukolsky, and W.T. Vetterling, *Numerical Recipes* (Cambridge University Press, Cambridge, 1986).
[23] D. Hardie and R.N. Parkins, Philos. Mag. **4**, 815 (1959).
[24] E. Wachowicz and A. Kiejna, J. Phys.: Condens. Matter **13**, 10 767 (2001).
[25] E. Ziambaras and E. Schröder, Phys. Rev. B **68**, 064112 (2003).
[26] A.R. Wazzan and L.B. Robinson, Phys. Rev. **155**, 586 (1967).
[27] H.L. Davis, J.B. Hannon, K.B. Ray, and E.W. Plummer, Phys. Rev. Lett. **68**, 2632 (1992).
[28] H.B. Michaelson, J. Appl. Phys. **48**, 4729 (1977).
[29] A. Kiejna and B.I. Lundqvist, Phys. Rev. B **63**, 085405 (2001).
[30] C.S. Fadley, in *Synchrotron Radiation Research: Advances in Surface Science*, edited by R.Z. Bachrach (Plenum, New York, 1990), Vol. 1.
[31] R. Fasel, P. Aebi, J. Osterwalder, L. Schlapbach, R.G. Agostino, and G. Chiarello, Phys. Rev. B **50**, 14 516 (1994).
[32] The multipole R factor R_{MP} is not a normalized quantity, therefore its absolute value depends on many parameters and only relative differences are significant for structural analysis. So far, no rigorous theory for error estimation has been developed for R_{MP}. It is our experience, however, that R-factor differences of 10% are significant and allow to safely rule out structures with higher R_{MP} values.